ORIGINAL ARTICLE

CME

Relationship between myocardial viability, myocardial blood flow and coronary anatomy by positron emission tomography integrated with multislice computed tomography

EMA N. ARAMAYO GERÓNIMO, AMÍLCAR R. OSORIO, RICARDO J. GERONAZZO[MTSAC], MAURO NAMÍAS, ROXANA CAMPISI [MTSAC]

Received: 12/29/2011
Accepted: 09/10/2012

Address for reprints:
Dra. Roxana Campisi
Nazca 3449 (1417)
Ciudad de Buenos Aires, Argentina

ABSTRACT

Background
The relationship between myocardial viability, myocardial blood flow and the degree of epicardial coronary stenosis in patients with coronary artery disease and left ventricular dysfunction is unclear.

Objective
The purpose of this study is to determine whether positron emission tomography (PET) viability patterns and myocardial flow at rest correlate with the degree of epicardial coronary stenosis.

Methods
Myocardial viability was evaluated in 27 patients by the combined analysis of ^{13}N-Ammonia ($^{13}NH_3$) perfusion and ^{18}F-2-fluoro-2-deoxyglucose (FDG) metabolism to identify four PET patterns: match (concordant reduced uptake of both radiotracers), mismatch (hypoperfusion with preserved FDG uptake), reverse mismatch (preserved perfusion and reduced FDG uptake) and preserved uptake of both radiotracers. Myocardial blood flow was calculated using a two-compartment model. Coronary artery stenosis was classified as mild (< 50%), moderate (>50%), severe (>70%) and critical (≥90%).

Results
In the 459 analyzed segments, 33% were match, 12% mismatch, 11% reverse-mismatch and 44% preserved patterns. Mismatch, reverse-mismatch and preserved patterns exhibited higher flows than the match pattern ($p<0.01$). Fifteen coronary lesions were mild, 7 moderate, 20 severe and 39 critical. There was no correlation between the degree of coronary stenosis and viability patterns ($R<0.2$, p=NS) or blood flow values ($R=0.12$). Analysis by vascular territory did not correlate with the degree of coronary stenosis (p=NS).

Conclusions
Lack of correlation between PET viability patterns, degree of epicardial stenosis and myocardial blood flow suggest that coronary anatomy can neither differentiate viable from necrotic myocardium nor predict the functional status of myocardial flow in patients with left ventricular dysfunction.

Rev Argent Cardiol 2013;81:113-118. http://dx.doi.org/10.7775/rac.v81.i2.737

Key words > Positron-Emission Tomography - Cell Survival - Perfusion Imaging

Abbreviations >

$^{13}NH_3$:	^{13}N-Ammonia	**PET:**	Positron emission tomography
CA:	Coronary angiography	**PRT/CT:**	Positron emission tomography integrated with multidetector computed tomography
CT:	Multidetector computed tomography		
FDG:	^{18}F-fluoro-2-deoxyglucose	**ROI:**	Regions of interest
LV:	Left ventricle	**RV:**	Right ventricle

SEE RELATED ARTICLE: http://doi.org/10.7775/rac.v81.i2.2498 Rev Argent Cardiol 2013;81:93-95

Fundación Centro Diagnóstico Nuclear
[MTSAC] Full member of the Argentine Society of Cardiology

BACKGROUND

Evaluation of glucose metabolism with ^{18}F-2-fluoro-2-deoxyglucose (FDG) by positron emission tomography (PET) is the most sensitive non-invasive technique for assessing myocardial viability. (1) FDG behaves as a glucose analogue, entering myocardial cells in direct proportion to coronary flow through glucose-specific protein channels (carriers) (GLUT-1 and GLUT-4). Then, FDG is uptaken by the carbohydrate metabolic pathway and phosphorylated by hexokinase to form FDG-6-phosphate. This process is proportional to the rate of myocardial glucose utilization at the time of injection, which depends on the metabolic state of the tissue. Once phosphorylated, FDG-6-phosphate remains in the cardiac myocite without further metabolic processing. Hence, FDG is a molecular marker of performance and of the balance between glucose transporters (membrane integrity) and hexokinase.

In the viable myocardium, the subsequent metabolism of the FDG-6-phosphate molecule is very slow, allowing sufficient intracellular retention for image interpretation. Conversely, in the presence of myocardial necrosis, FDG uptake is greatly decreased or even absent. (2) To assess myocardial viability, most studies compare myocardial perfusion with flow radiotracers as nitrogen-13-ammonia ($^{13}NH_3$) or myocardial FDG uptake with rubidium-82 (82Rb). (3) The combination of these two radiotracers can be used to determine the relationship between flow and metabolism, identifying with greater specificity both viable myocardium (including stunning and hibernation) and necrotic myocardium in patients with left ventricular dysfunction caused by coronary disease. (4) Assessment of perfusion with $^{13}NH_3$, also allows quantification of absolute myocardial blood flow (ml / min / g) in a single study, without further radiation exposure to the patient. (5) In the search for the best therapeutic decision, integrated assessment of these patients usually associates myocardial viability studies with information of coronary anatomy by coronary angiography (CA).

The aim of this study is to investigate the relationship between PET patterns of myocardial viability, myocardial blood flow and the degree of epicardial coronary stenosis in patients with ventricular dysfunction caused by coronary artery disease.

METHODS

Study population

The study included 50 patients with dilated cardiomyopathy of coronary etiology and severe left ventricular (LV) dysfunction, referred for myocardial viability evaluation with combined PET-multidetector computed tomography (PET/CT). Twenty seven patients with CA within six months of PET study were retrospectively selected. All patients signed the informed consent form for the clinical study.

PET protocol

Patients were positioned in a hybrid Discovery STE/CT system for the myocardial perfusion study. Heart rate, arterial blood pressure and electrocardiogram were continuously monitored. First, a thoracic scan (CT scout) was performed, including the cardiac region for CT and PET acquisition. This was followed by a low-dose CT scan (CTDI < 2 mGY) synchronized with the gating signal for subsequent attenuation correction. Then, 0.17 mCi/kg (average 15mCi or 555 MBq) of $^{13}NH_3$ were injected with a perfusion pump. Acquisition in list mode was synchronized with the radiotracer injection. Dynamic acquisition in 2D mode [12 frames x 10s, 3 x 20s, 4 x 30s and 2 frames x 300s] was initiated simultaneously with the radiotracer injection. After the first three minutes, a static and a gated series were obtained, followed by a 5-minute gated sequence in 3D mode.

To assess metabolism, the patients came on the second day in fasting conditions. After confirming basal blood glucose level < 160 mg/dl, an oral load of glucose (50 gr) was administered. Subsequent serial blood glucose measurements were performed, and according to a pre-established protocol, intravenous insulin was administered to optimize myocardial glucose uptake. After verifying myocardial substrate change from fatty acids to glucose (when blood glucose level was < 150 mg/dl), 0.11 mCi/kg (average 10 mCi or 370 MBq) FDG was injected. Sixty minutes after the injection, 3D mode static and gated image acquisition was initiated. (600 s acquisition in 8 bins), and completed with a low dose CT scan (CTDI) < 2mGY) for attenuation correction.

All patients were studied without modification of their usual pharmacological treatment.

Analysis of PET images

Studies were processed in a GE-Xeleris® workstation. First, short-axis transaxial images were reoriented in slices perpendicular to the long base-apex axis, a vertical long axis in vertical slices from the septum to the lateral wall and a horizontal long axis in horizontal slices from the inferior to the anterior wall. Correct alignment was performed between PET emission images and CT transmission images for attenuation correction.

The LV was divided into 17 segments (6) to analyze perfusion and metabolic images (Figure 1A).

To perform the semiquantitative analysis, FDG uptake was normalized to the highest $^{13}NH_3$ uptake in the regions with normal myocardial flow. Visual analysis consensus from two trained observers assigned a 0-4 score to each segment according to the degree of radiotracer uptake, both for perfusion as metabolic images. A 0 score corresponded to the preserved tracer uptake, 1 mild, 2 moderate, 3 severe decrease of tracer uptake and 4 absence of tracer uptake. Segments were classified according to the combined assessment of perfusion and metabolism into 4 PET viability patterns, following nuclear cardiology procedure guidelines (4) (Figure 1B):

1. **Match:** concordant reduced uptake of both radiotracers, indicative of necrotic myocardium
2. **Mismatch:** reduced $^{13}NH_3$ uptake discordant with pre served FDG uptake, denoting myocardial hibernation
3. **Preserved:** preserved uptake of both radiotracers in the presence of contractile dysfunction
4. **Reverse mismatch:** preserved $^{13}NH_3$ uptake, discord ant with reduced FDG uptake, indicative of viable myo cardium (this pattern is observed in myocardial stun ning, left bundle branch block, diabetes mellitus and/or multivessel disease). (7)

Myocardial flow at rest was calculated from dynamic $^{13}NH_3$ images, using Carimas 2.0 software. (8) Transaxial images were reoriented into the three conventional axes, and regions of interest (ROI) were automatically defined in the myocardium, the left ventricular vascular pool and in the right ventricle (RV). Regions of interest determined au-

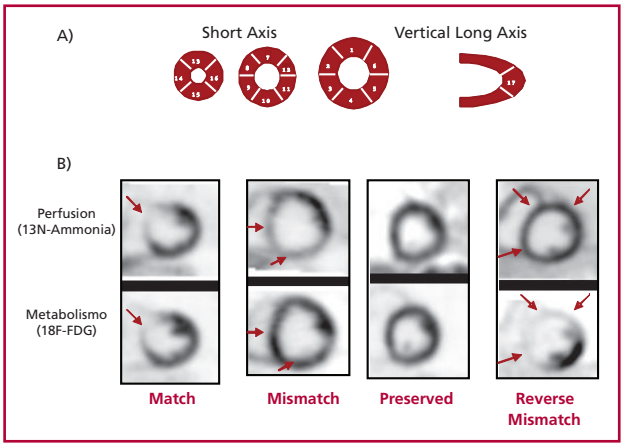

Fig. 1. Left ventricular segmentation and myocardial viability patterns. **A.** Seventeen-segment model based on three short-axis slices: apical, medial and basal and a vertical long axis slice. Basal, medial and apical anterior (1, 7, 13), basal and medial anteroseptal (2, 8), septoapical (14) and apical (17) segments correspond to the anterior descending coronary artery territory. Basal and medial anterolateral (6, 12), basal and medial inferolateral (5, 11) and lateroapical segments correspond to the circumflex coronary artery, and basal and medial (4, 10), basal and medial inferoseptal (3, 9) and inferoapical (15) to the right coronary artery territory. **B.** PET patterns of myocardial viability resulting from the combined analysis of 13N-ammonia perfusion and 18F-FDG metabolism.

tomatically by the program were manually corrected. Then, activity curves as a function of time were obtained for the left anterior descending, circumflex and right coronary artery territories, in each of the 17 segments as well as in the left ventricular and right ventricular vascular pool. Activity-time curves were adjusted to a previously validated two-compartment mathematical model of $^{13}NH_3$ kinetics, (9-11) which allows the calculation of myocardial flow at rest in ml/min/g for each of the four patterns of myocardial viability identified by PET.

Gated PET: the Emory Toolbox® software was used to calculate ejection fraction, ventricular volumes, wall motion and left ventricular systolic thickening from gated images.

Coronary angiography

Coronary angiography reports were evaluated and lesions were classified according to the percentage of coronary obstruction as: mild (< 50%), moderate (50 to 70%), severe (> 70%) and critical (> 90%).

Statistical analysis

Continuous variables were expressed as mean, standard deviation and median. Match results were compared with the group formed by the rest of the patterns using Student´s test. A p value < 0.05 was considered statistically significant. Pearson´s correlation coefficient was used to evaluate the correlation coefficient between PET patterns and the degree of epicardial coronary stenosis. This correlation analysis was chosen over Spearman´s test because the hypothesis testing is more accurate for large samples.

RESULTS

Population characteristics are described in Table 1. In the 459 segments of 27 study patients, 33% presented match pattern, 12% mismatch, 11% reverse mismatch and 44% preserved perfusion and metabolism (Table 2).

According to CA results, 15 stenoses were mild, 7 moderate, 20 severe and 39 critica

Myocardial blood flow at rest according to the different patterns

From a total of 459 segments, 11 segments were discarded due to partial volume effect affecting adequate myocardial flow quantification. Average flow was calculated in the remaining 448 segments for each PET pattern. Mean flow for the match pattern was 0.39 ml/min/g, significantly lower than the mismatch pattern flow of 0.50 ml/min/g. Reverse mismatch presented an average flow of 0.61 ml/min/g and the preserved pattern flow was 0.69 ml/min/g ($p < 0.01$) (see Table 2).

Relationship between the degree of coronary stenosis and the incidence of the different PET patterns

There was no correlation between the degree of epicardial coronary stenosis and the different PET viability patterns (RPearson > 0.2), both in the overall analysis as in the analysis of each vascular territory. This is shown in Figure 2, where for each obstruction degree different percentages of PET patterns can be seen. This means that in presence of epicardial disease, regardless the degree of coronary stenosis, neither the presence nor abscense of necrosis nor viable myocardium can be predicted, and in the case of viable whether it is hibernated or stunned.

Relationship between the degree of coronary stenosis and myocardial blood flow at rest

Table 1. Clinical characteristics of the population

Age (years)	59 ± 11
BMI (kg/m2)	27± 5
Left ventricular ejection fraction, %	29 ± 11
Male gender	22
Coronary risk factors	
Hypertension, n	19
Dyslipidemia, n	21
Smoking, n	6
Ex smoker, n	7
Diabetes mellitus, n	
Others	3
Left bundle branch block, n	5
Pacemaker, n	2
Symptoms, n	12
Dyspnea, n	6
Angina, n	6
Coronary angioplasty, n	3
Anterior Q wave myocardial infarction, n	20
Inferior Q wave myocardial infarction, n	3
Non-Q wave myocardial infarction, n	2
Revascularization surgery, n	1

BMI: Body mass index

Absolute values of myocardial blood flow at rest for each segment were variable and scattered for each degree of coronary stenosis. There was no correlation between epicardial coronary stenosis and blood flow at rest for each segment (R=0.12) The analysis by vascular territory showed no correlation of myocardial blood flow at rest with the degree of epicardial coronary stenosis (p= NS). Only the analysis of the viable patterns presented a slight, though not significant, decrease in the median of absolute flow at rest with greater degree of coronary stenosis.

DISCUSSION

The main result of this study is that the incidence of PET/CT myocardial viability patterns and myocardial blood flow at rest values were independent of the location and degree of epicardial coronary stenosis in patients with left ventricular dysfunction caused by coronary artery disease.

Combined analysis of PET myocardial perfusion and metabolism can discern both viable and necrotic myocardium with greater specificity than isolated evaluation of metabolism. (3) In patients with severe reduction of left ventricular contractility, the positive predictive value for improved contractile function with revascularization is 76% and the negative predictive value is 82%. (12)

Published data indicate that the visual analysis of reduced regional tracer uptake and software semiquantitative analysis have similar diagnostic accuracy for detecting viable myocardium. (13) In this study, the segments were analyzed using a visual score according to the guidelines of the American Society of Nuclear Cardiology. The segments were categorized into four PET patterns that differentiated myocardial necrosis from myocardial viability. All metabolic studies were performed standardizing the patient's diet after an oral glucose load to favor the change of myocardial metabolism from fatty acids to glucose. In addition, all images had attenuation correction and were normalized to the myocardial segment which exhibited the best perfusion. (4) Therefore, the categorization of the four segments in PET patterns cannot be attributed to patient diet variations or technical problems.

For each PET pattern, myocardial blood flow at rest was quantified in absolute values by dynamic imaging with $^{13}NH_3$. (14) Uptake of perfusion tracer depends on blood flow and tissue retention (metabolic component).As these two factors cannot be separated by the analysis of static images, it is necessary to use compartment kinetic models. (15) In our group of patients, there was a significant correlation between the four PET patterns and blood flow, which was sig-

Table 2. Incidence of PET viability patterns and myocardial blood flow at rest

Pattern	Nº of segments (n = 448)	Coronary blood flow at rest (ml/min/g)
Match	153 (33%)	0.39 ± 0.2*
Mismatch	55 (12%)	0.50 ± 0.3
Reverse mismatch	49 (11%)	0.61 ± 0.2
Preserved	202 (44%)	0.69 ± 0.2

Notice that blood flow at rest in the match pattern was significantly lower than that of viable segments, *p<0.05. PET: Positron emission tomography

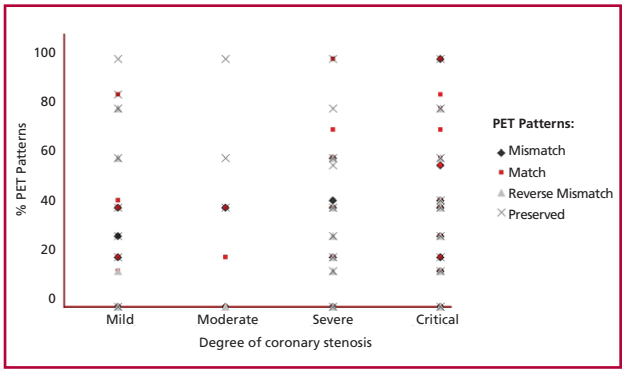

Fig. 2. Relationship between PET patterns and the degree of epicardial coronary stenosis. The extent of PET patterns was highly variable for each degree of lesion. There was no correlation between the incidence of each pattern and the degree of epicardial coronary stenosis. Note, for example, that the match pattern can be seen at any degree of stenosis, as well as for the rest of the PET patterns.

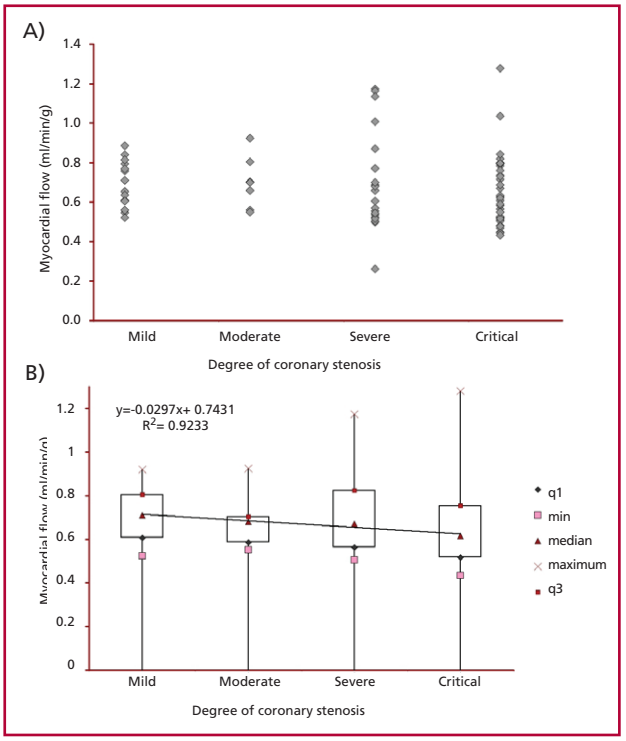

Table 2. Relationship between myocardial flow at rest and epicardial coronary stenosis. **A.** Values of myocardial flow at rest were different for each degree of coronary stenosis. **B.** The viable segments presented a slight, though not significant, decrease in the median value of absolute blood flow at rest with greater degree of stenosis (slope=0.04, R=-0.96), consistent with lack of correlation between stenosis severity and viability patterns (q1: quartile 1; q3: quartile 3).

nificantly higher in viable than in necrotic territories. Beanlands et al. (16) demonstrated that coronary flow at rest in necrotic segments is ≤ 0.45 ml/min/g whereas in viable segments it is > 0.45 ml/min/g. In the present study, mean blood flow in the necrotic myocardium was 0.39 ml/min/g, in accordance with results reported in the literature. (11) Our group had previously reported that using a cutoff value of 0.47 ml/min/g, the sensitivity and specificity to qualify tissue viability is 83%. (17)

The complexity to perform and analyze dynamic studies with $^{13}NH_3$, added to its short half-life (10 minutes), limits its use to centers possessing on-site cyclotron adjacent to the PET. This hinders the performance of large scale studies, necessary to evaluate whether the images acquired with the single administration of $^{13}NH_3$ have prognostic value in patients with left ventricular dysfunction. It is noteworthy that currently, the prognostic value of viability studies with PET is given by the presence or absence of mismatch and match patterns.

Structural indexes, as the percent obstruction of an epicardial coronary artery, often differ from functional parameters. This discrepancy between anatomy and microvascular function is multifactorial and may depend on the length of the stenosis, on its eccentricity, on collateral circulation or on the presence of endothelial dysfunction, among others. (5) In this group of patients, there was no correlation between coronary flow at rest and degree of epicardial coronary stenosis. When only the flows of viable segments were analyzed, there was a slight, but not significant, decrease in the median of absolute flow with greater degree of stenosis. These results suggest that a specific epicardial coronary stenosis cannot predict the degree of microcirculatory involvement at rest.

When we analyzed the relationship of the four PET myocardial viability patterns and the percentage of coronary stenosis we did not find a significant correlation. It is of interest that this lack of correlation was independent of the analyzed coronary vessel.

Limitations

A limitation of our study was the lack of evaluation of collateral circulation and its potential correlation with viability patterns. This was analyzed by Di Carli et al., (18) who described that the visualization of collateral circulation in myocardial regions supplied by occluded arteries does not always imply presence of viable myocardium. In fact, collateral visualization was a non-specific mismatch pattern marker. Moreover, lack of collateral circulation did not necessarily mean low probability of viable myocardium.

Another limitation of our study is that the findings emerge from our database analysis. Nevertheless, they have clinical relevance.

CONCLUSIONS

Sometimes the coronary angiography information alone can define the indication of revascularization in patients with coronary artery disease and left ventricular dysfunction. Yet, as described, the degree and location of epicardial coronary stenosis does not predict the presence or absence of myocardial viability. Therefore, in selected patients, we believe that the integration of clinical, anatomical, functional and metabolic information is necessary in decision-making. Further studies are needed to determine the impact of integrated information after revascularization, taking into account that its success depends not only on functional recovery, but also on improving survival, increasing exercise capacity, reverting left ventricular remodeling and preventing sudden death.

RESUMEN

Relación entre los patrones de viabilidad miocárdica, el flujo miocárdico y la anatomía coronaria en pacientes con disfunción ventricular izquierda, evaluada mediante tomografía por emisión de positrones integrada con tomografía computarizada multicorte

Introducción
La relación entre la viabilidad, el flujo miocárdico y el grado de estenosis epicárdica en pacientes con enfermedad coronaria y disfunción ventricular izquierda está poco investigada.

Objetivo
Determinar si los patrones de viabilidad por tomografía por emisión de positrones (PET) y el flujo miocárdico en reposo se relacionan con el grado de estenosis epicárdica.

Material y métodos
Se evaluó la viabilidad en 27 pacientes mediante el análisis combinado de la perfusión con ^{13}N-amonio ($^{13}NH_3$) y el metabolismo con ^{18}F-2-fluoro-2-desoxiglucosa (FDG) para identificar cuatro patrones PET: match (hipocaptación concordante de ambos radiotrazadores), mismatch (hipoperfusión con captación preservada de FDG), mismatch inverso (perfusión preservada e hipocaptación de FDG) y perfusión/metabolismo conservados. El flujo absoluto se calculó mediante un modelo bicompartimental. Las estenosis se clasificaron en leves (< 50%), moderadas (> 50%), graves (> 70%) y críticas (≥ 90%).

Resultados
De 459 segmentos resultaron match el 33%, mismatch el 12%, mismatch inverso el 11% y conservado el 44%. El flujo para mismatch, mismatch inverso y conservado fue mayor que para los segmentos con match (p < 0,01). Quince lesiones fueron leves, 7 moderadas, 20 graves y 39 críticas. No hubo correlación entre el grado de estenosis y los patrones de viabilidad (R < 0,2; p = ns) ni con los valores de flujo (R = 0,12). El análisis por territorio vascular no mostró correlación con el grado de estenosis (p = ns).

Conclusiones
No hubo correlación entre los patrones PET, el grado de estenosis epicárdica y el flujo miocárdico, lo que sugiere que la anatomía coronaria no puede discriminar miocardio viable del necrótico ni predecir el estado del flujo miocárdico en pacientes con disfunción ventricular izquierda.

Palabras clave > Tomografía por emisión de positrones - Supervivencia celular - Imagen de perfusión

Conflicts of interest
None declared.

Acknowledgements
To radiologists of the Fundación Centro Diagnóstico Nuclear: Dr. Gabriel Bruno, Yamila B and Christian González, PET / CT technicians: Lucio De Blumenkrantz Innocentiis and Soledad González, and to all the members of the radiopharmacy and cyclotron area, specially Alicia Coronel and Adrian Durán.

REFERENCES

1. Saraste A, Ukkonen H, Kajander S, Knuuti J. Integrated anatomy and viability PET-CT. EuroIntervention 2010;6:G132-7.
2. Tillisch J, Brunken R, Marshall R, Schwaiger M, Mandelkern M, Phelps M, et al. Reversibility of cardiac wall-motion abnormalities predicted by positron emission tomography. E Engl J Med 1986;314:884-8. http://doi.org/ckk6qs
3. Knuuti J, Schelbert HR, Bax JJ. The need for standardisation of cardiac FDG PET imaging in the evaluation of myocardial viability in patients with chronic ischaemic left ventricular dysfunction. Eur J Nucl Med Mol Imaging 2002;29:1257-66. tp://doi.org/chh7hv
4. Dilsizian V, Bacharach SL, Beanlands RS, Bergmann SR, Delbeke D, Gropler RJ, Knuuti J, Schelbert HR, Travin MI. PET myocardial perfusion and metabolism clinical imaging. ASNC imaging guidelines for nuclear cardiology procedures. J Nucl Cardiol 2009. http://doi.org/bhrfnx
5. Schelbert HR. Anatomy and physiology of coronary blood flow. J Nucl Cardiol 2010;17:545-54. http://doi.org/fdk67m
6. Cerqueira M, Weissman N, Dilsizian V, Jacobs A, Kaul S, Laskey W, et al. Standardized Myocardial Segmentation and Nomenclature for Tomographic Imaging of the heart: a statement for healthcare professionals from the Cardiac Imaging Committee of the Council on Clinical Cardiology of the American Heart Association. Circulation 2002;105:539-42. http://doi.org/dxz8tw
7. Machac J, Bacharach L, Bateman TM, Bax JJ, Beanlands R, Bengel F, et al. Positron emisión tomography myocardial perfusion and glucose metabolism imaging. J Nucl Cardiol 2006;13:e121-51. http://doi.org/ctssk6
8. Carimas 2.0, © Turku PET Centre. http://www.turkupetcentre.net/carimasturku/
9. DeGrado TR, Hanson MW, Turkington TG, Delong DM, Brezinski DA, Vallee JP, et al. Estimation of myocardial blood flow for longitudinal studies with 13N-labeled ammonia and positron emission tomography. J Nucl Cardiol;3:494-507. http://doi.org/fsg2wq
10. Namagachi S, Czernin J, Kim AS, Sun KT, Böttcher M, Phelps ME, et al. Reproducibility of measurementes of regional resting and hiperemic myocardial blood flow assessed with PET. J Nucl Med 1996;37:1626-31.
11. Muzik O, Beanlands RS, Hutchins GD, Manger Tj, Nguyen n, Schwaiger M. Validation of nitrogen 13-ammonia tracer kinetic model for quantification of myocardial blood flow using PET. J Nucl Med 1993;34:83-91.
12. Di Carli MF. Predicting improved function after myocardial revascularization. Curr Opin Cardiol 1998;13:415-24. http://doi.org/brf2sb
13. Hesse B, Taegil K, Cuocolo A, Anagnostopoulos G, Bardiés M, Bax J, et al; EANM/ESC Group. EANM/ESC procedural guidelines for myocardial perfusion imaging in nuclear cardiology. Eur J Nuc Med Mol Imaging 2005;32:855-97. http://doi.org/d3fss4
14. Ziadi MC, deKemp RA, Beanlands RS. Quantification of myocardial perfusion: What will it take to make it to prime time? Current Cardiovascular Imaging Reports 2009;2:238–49. http://doi.org/bdm7nc
15. Gerwitz H, Fischman AJ, Abraham S, Gilson M, Strauss HW, Alpert NM. Positron emission tomographic measurements of absolute regional myocardial blood flow permits indentification of nonviable myocardium in patients with chronic myocardial infarction. J Am Coll Cardiol 1994;23:851-9. http://doi.org/bq5tn8
16. Beanlands RS, deKemp RA, Scheffel A, Nahmias C, Garnett S, Coates ,G et al. Can nitrogen-13 Ammonia kinetic modeling define myocardial viability independent of Fluorine-18 fluorodeoxyglucose? J Am Coll Cardiol 1997;29:537-43. http://doi.org/bkb4qw
17. Geronazzo RJ, Osorio AR, Bruno G, Namías M, Campisi R. Comparación entre flujo absoluto miocárdico determinado con N-13 Amonio y viabilidad miocárdica con F-18-2-Desoxiglucosa valorado mediante PET/TC. Rev Argent Cardiol. 2009;77:121.
18. Di Carli MF, Sherman T, Kahnna S, Davidson M, Rokhsar S, Hawkins R, et al. Myocardial viability in asynergic regions subtended by occluded coronary arteries: relation to the status collateral flow in patients with chronic coronary artery disease. J Am Coll Cardiol 1994;23:860-8.